

UCLA

UCLA Previously Published Works

Title

Diffusion MRI Phenotypes Predict Overall Survival Benefit from Anti-VEGF Monotherapy in Recurrent Glioblastoma: Converging Evidence from Phase II Trials

Permalink

<https://escholarship.org/uc/item/4vp1521c>

Journal

Clinical Cancer Research, 23(19)

ISSN

1078-0432

Authors

Ellingson, Benjamin M
Gerstner, Elizabeth R
Smits, Marion
[et al.](#)

Publication Date

2017-10-01

DOI

10.1158/1078-0432.ccr-16-2844

Peer reviewed



Published in final edited form as:

Clin Cancer Res. 2017 October 01; 23(19): 5745–5756. doi:10.1158/1078-0432.CCR-16-2844.

Diffusion MRI phenotypes predict overall survival benefit from anti-VEGF monotherapy in recurrent glioblastoma: Converging evidence from phase II trials

Benjamin M. Ellingson, Ph.D.^{1,2,3}, Elizabeth R. Gerstner, M.D.⁴, Marion Smits, M.D., Ph.D.⁹, Raymond Y. Huang, M.D.¹¹, Rivka Colen, M.D.¹², Lauren E. Abrey, M.D.⁵, Dana T. Aftab, Ph.D.⁶, Gisela M. Schwab, M.D.⁶, Colin Hessel, M.S.⁶, Robert J. Harris, Ph.D.^{1,2}, Ararat Chakhoyan, Ph.D.^{1,2}, Renske Gahrman, M.D.⁹, Whitney B. Pope, M.D., Ph.D.², Kevin Leu, Ph.D.^{1,2}, Catalina Raymond, M.S.^{1,2}, Davis C. Woodworth, B.S.^{1,2}, John de Groot, M.D.¹³, Patrick Y. Wen, M.D.⁸, Tracy T. Batchelor, M.D.⁴, Martin J. van den Bent, M.D.¹⁰, and Timothy F. Cloughesy, M.D.^{3,7}

¹UCLA Brain Tumor Imaging Laboratory (BTIL), Center for Computer Vision and Imaging Biomarkers, David Geffen School of Medicine, University of California Los Angeles, Los Angeles, CA ²Dept. of Radiological Sciences, David Geffen School of Medicine, University of California Los Angeles, Los Angeles, CA ³UCLA Neuro Oncology Program, David Geffen School of Medicine, University of California Los Angeles, Los Angeles, CA ⁴Massachusetts General Hospital Cancer Center, Boston, MA ⁵F. Hoffman-La Roche, Ltd ⁶Exelixis, South San Francisco, CA ⁷Dept. of Neurology, David Geffen School of Medicine, University of California Los Angeles, Los Angeles, CA ⁸Center for Neuro-Oncology, Dana-Farber/Brigham and Women's Cancer Center, Harvard Medical School, Boston, MA ⁹Department of Radiology and Nuclear Medicine, Erasmus MC - University Medical Centre Rotterdam, The Netherlands ¹⁰Department of Neuro-Oncology, Erasmus MC - University Medical Centre Rotterdam, The Netherlands ¹¹Department of Radiology, Brigham and Women's Hospital, Boston, Massachusetts ¹²Department of Neuroradiology, University of Texas M.D. Anderson Cancer Center, Houston, TX, USA ¹³Department of Neuro-Oncology, University of Texas M.D. Anderson Cancer Center, Houston, TX, USA

Abstract

Purpose—Anti-VEGF therapies remain controversial in the treatment of recurrent glioblastoma (GBM). In the current study we demonstrate that recurrent GBM patients with a specific diffusion MR imaging signature have an overall survival (OS) advantage when treated with cediranib,

Address Correspondence to: Benjamin M. Ellingson, Ph.D., Director, UCLA Brain Tumor Imaging Laboratory (BTIL), Associate Professor of Radiology, Biomedical Physics, Psychiatry, and Bioengineering, Departments of Radiological Sciences and Psychiatry, David Geffen School of Medicine, University of California, Los Angeles, 924 Westwood Blvd., Suite 615, Los Angeles, CA 90024 (bellingson@mednet.ucla.edu), Phone: 310-481-7572, Fax: 310-794-2796.

Conflicts of Interest related to this Manuscript: Benjamin M. Ellingson, Albert Lai, Tracy Batchelor, and Timothy F. Cloughesy are paid consultants, members of the advisory board, and are research grant recipients from Roche/Genentech. Lauren E Abrey is an employee of Roche/Genentech. Dana T. Aftab, Gisela M. Schwab, and Colin Hessel are paid employees and stockholders for Exelixis. Tracy Batchelor is a consultant for Merck, Proximagen/Upsher, Oxigene, Cavion, and Accerta and has research support from Pfizer. Martin van den Bent has received research support from Roche. Marion Smits is a paid independent reviewer for Parexel.

bevacizumab, cabozantinib, or aflibercept monotherapy at first or second recurrence. These findings were validated using a separate trial comparing bevacizumab with lomustine.

Experimental Design—Patients with recurrent GBM and diffusion MRI from the monotherapy arms of 5 separate Phase II clinical trials were included: 1) cediranib (NCT00035656); 2) bevacizumab (BRAIN Trial, AVF3708g; NCT00345163); 3) cabozantinib (XL184-201; NCT00704288); 4) aflibercept (VEGF Trap; NCT00369590); and 5) bevacizumab or lomustine (BELOB; NTR1929). Apparent diffusion coefficient (ADC) histogram analysis was performed prior to therapy to estimate “ADC_L”, the mean of the lower ADC distribution. Pre-treatment ADC_L, enhancing volume, and clinical variables were tested as independent prognostic factors for OS.

Results—The coefficient of variance (COV) in double baseline ADC_L measurements was 2.5% and did not significantly differ (P=0.4537). An ADC_L threshold of 1.24 um²/ms produced the largest OS differences between patients (HR~0.5) and patients with an ADC_L>1.24 um²/ms had close to double the OS in all anti-VEGF therapeutic scenarios tested. Training and validation data confirmed baseline ADC_L was an independent predictive biomarker for OS in anti-VEGF therapies, but not lomustine, after accounting for age and baseline enhancing tumor volume.

Conclusions—Pre-treatment diffusion MRI is a predictive imaging biomarker for OS in patients with recurrent GBM treated with anti-VEGF monotherapy at first or second relapse.

Keywords

Diffusion MRI; ADC Histogram Analysis; T1 subtraction; recurrent glioblastoma; bevacizumab; cediranib; cabozantinib

INTRODUCTION

Glioblastoma (GBM) is the most common and lethal type of primary brain tumor in adults. Median survival for patients diagnosed with a GBM is around 14 months,(1) and fewer than 10% of patients survive beyond 5 years after diagnosis.(2) The current standard of care for newly diagnosed GBM consists of maximum safe surgical resection, followed by radiotherapy plus concomitant and adjuvant temozolomide. At recurrence, however, few effective therapeutic options exist, and median survival is only around 8–10 months (3–5).

High tumor vascularity resulting from elevated production of pro-angiogenic growth factors, including vascular epithelial growth factor (VEGF)(6, 7), has led to the development of therapies targeting pro-angiogenic signaling pathways(8). Anti-angiogenic therapies that specifically target VEGF and its receptors fall into two general categories: antibodies or tyrosine kinase inhibitors (TKIs) (9). Bevacizumab, a humanized monoclonal antibody for VEGF-A (Fig 1), was approved for use in recurrent GBM in 2009 after it was shown to improve progression-free survival (5, 10). Bevacizumab is often used for the treatment of recurrent GBM and almost all patients will receive bevacizumab at some point during their treatment. Aflibercept, or “VEGF trap”, is a recombinant fusion protein that has been tested in recurrent GBM(11) and similarly acts in the extracellular domain by trapping VEGF through use of VEGF-binding portions from the extracellular domains of VEGFR-1 and VEGFR-2. Cediranib and cabozantinib, which are both multi-targeted pan-VEGF receptor

TKIs (12–17), have also been studied as promising anti-angiogenic agents that inhibit different aspects of VEGF signaling, specifically the intracellular kinase domain of the VEGF receptors (Fig 1).

Despite promising initial data and widespread exploration of anti-VEGF therapies in recurrent GBM, randomized phase II trials have not demonstrated an overall survival (OS) benefit for un-selected patients with recurrent GBM. However, recent evidence suggests certain subsets of patients with specific imaging characteristics may have a significant OS benefit from anti-VEGF therapy. For example, single and multi-center studies have shown that high pre-treatment apparent diffusion coefficient (ADC) measured with diffusion MRI within the contrast enhancing portion of the tumor is a significant and independent predictor of prolonged OS in patients treated with bevacizumab (18–21). Since bevacizumab, cediranib, cabozantinib, and aflibercept are all VEGF pathway inhibitors, and all commonly have activity against VEGFR-2, we hypothesized baseline diffusion MRI characteristics in recurrent GBM may be predictive of survival benefit for all four anti-VEGF therapies. Thus, the purpose of this study was to first evaluate whether pre-treatment diffusion MR measurements of ADC within the contrast enhancing tumor is an independent, significant predictor of OS benefit in recurrent GBM patients treated with anti-VEGF monotherapy by examining data in a series of multicenter, phase II trials in cediranib monotherapy (NCT00035656), bevacizumab monotherapy (BRAIN Trial, AVF3708g; NCT00345163), cabozantinib monotherapy (XL184-201; NCT00704288), and aflibercept monotherapy (VEGF trap, NABTC0601; NCT00369590). Lastly, we validated our findings in an independent cohort of recurrent GBM patients treated with bevacizumab monotherapy versus lomustine monotherapy (BELOB), confirming that diffusion MR phenotypes are exclusively predictive for anti-VEGF therapy.

METHODS

Patient Population

A total of 258 anti-VEGF treatment naïve recurrent GBM patients with measurable enhancing tumor ($>1\text{cm}^3$) and adequate diffusion MRI estimates of apparent diffusion coefficient (ADC) available from 5 separate phase II clinical trials were included in this study. Data from four trials were used as training cohorts: 1) 30 patients treated with cediranib monotherapy (NCT00035656), including two pre-treatment (double baseline) MR examinations; 2) 57 patients treated with bevacizumab monotherapy (BRAIN Trial, AVF3708g; NCT00345163); 3) 65 patients treated with cabozantinib monotherapy (XL184-201; NCT00704288); 4) 25 patients treated with aflibercept monotherapy (VEGF trap; NABTC0601; NCT00369590); and one trial was used for validation: 5) 42 patients treated with bevacizumab monotherapy and 39 patients treated with lomustine monotherapy as part of a phase II validation cohort (BELOB).

Disease progression that led to enrollment in each study was identified on MRI 14 days before the baseline treatment. All patients on all trials failed initial standard of care including concurrent radiotherapy and temozolomide and were required to be at least 8 weeks from completion of radiation therapy before considered eligible for each trial. Karnofsky performance status (KPS) was required to be ≥ 60 for all trials. Patients receiving

corticosteroids were required to be on stable or decreasing dose for at least 5 days prior to the baseline scan. All patients enrolled in all trials signed institutional review board-approved written consent at the respective study sites. Table 1 further outlines patient demographic information for each trial included in the current study.

Cediranib Monotherapy

A total of 30 patients of the 31 enrolled in an NCI-sponsored Phase II trial of cediranib, a pan-VEGF receptor TKI with additional activity against cKIT and PDGF β , at the Massachusetts General Hospital and Dana-Farber Cancer Institute, (NCI; NCT00035656) were included in the current study based on availability of high quality diffusion MR and anatomic data. One patient was excluded based on limited drug exposure, as described previously(22). Patients were treated with cediranib (AZD2171; AstraZeneca Pharmaceuticals, Cheshire, United Kingdom) at 45mg once daily on a 28-day cycle. For more information on the trial, therapeutic dosing information, and details on inclusion and exclusion criteria, see the following website for the trial: clinicaltrials.gov/ct2/show/NCT00035656 and final published clinical trial information from Batchelor *et al.*(22).

Bevacizumab Monotherapy

A total of 57 recurrent, histologically confirmed GBM patients within the bevacizumab monotherapy arm in the BRAIN trial (La Roche/Genentech, AVF3708g; NCT00345163), an open-label, multicenter (11 sites), randomized, noncomparative phase II trial performed to assess the effectiveness of bevacizumab or bevacizumab and irinotecan hydrochloride with or without concomitant enzyme-inducing antiepileptic drugs were included in the current study based on availability of both high quality diffusion and anatomic MRI at baseline. Patients within the bevacizumab monotherapy arm were treated with a dose of 10mg/kg every 2 weeks. Patients within the bevacizumab and irinotecan combination arm were not included in the current study. For more information on the trial, therapeutic dosing information, and details on inclusion and exclusion criteria, see the following website for the trial: clinicaltrials.gov/ct2/show/NCT00345163 and final published clinical trial information from Friedman *et al.*(5) (It is important to note that a previous study similar to the current study was already published using this dataset (20), but all data has been independently reanalyzed using slightly different methodology in the current study.)

Cabozantinib Monotherapy

A total of 65 anti-VEGF treatment naïve, recurrent GBM patients of the 152 originally enrolled as part of XL184-201, a multicenter (8 sites), phase II, open-label, uncontrolled study of cabozantinib (XL184; Exelixis; NCT00704288), a tyrosine kinase inhibitor with principal targets of MET, VEGF receptors, AXL, and RET, at a dose of 140 or 100 mg (free base equivalent weight, oral, daily) at first or second relapse were included in the current study based on availability of diffusion and anatomic imaging data. Specific inclusion and exclusion criteria for this trial can be found at clinicaltrials.gov/ct2/show/NCT00704288.

Aflibercept Monotherapy

A total of 25 patients with histologically confirmed GBM with evidence of unequivocal progression after chemoradiation enrolled in a NABTC and NCI sponsored multicenter (7 sites), phase II study of aflibercept (VEGF trap; NABTC0601; NCT00369590) were included in the current study based on availability of diffusion and anatomic imaging data. Patients were treated with a dose of 4mg/kg intravenously every 2 weeks. For more information on the trial, therapeutic dosing information, and details on inclusion and exclusion criteria, see the following website for the trial: clinicaltrials.gov/ct2/show/NCT00369590 and final published clinical trial information from de Groot *et al.*(11)

Single-Agent Bevacizumab versus Lomustine Monotherapy

To confirm that diffusion MR phenotypes are predictive of response to anti-VEGF therapies but *not* cytotoxic chemotherapies, we examined a total of 81 recurrent GBM patients treated with either bevacizumab monotherapy (N=42; 10mg/kg every 2 weeks) or lomustine (N=39; 110mg/m² every 6 weeks) as part of a multicenter (14 sites), Dutch investigator initiated phase II trial exploring bevacizumab, lomustine, or bevacizumab plus lomustine in patients with GBM at first recurrence (BELOB; NTR1929). Patients treated with combination bevacizumab and lomustine were not included in the current study. For more information on the trial, therapeutic dosing information, and details on inclusion and exclusion criteria, see the final published clinical trial information from Taal *et al.*(23)

Anatomic and Diffusion MRI Acquisition

Standard and diffusion MR data were acquired using either a 1.5T or a 3T MR scanner from an MR scanner manufactured by Siemens Healthcare (Erlangen, Germany), Philips Medical Systems (Best, the Netherlands), GE Medical Systems (Waukesha, Wisconsin), or Hitachi Medical Corporation (Tokyo, Japan). The MRI parameters for cediranib (24–26), bevacizumab (20, 27), and cabozantinib (28) trials have been published previously. T1-weighted images were acquired using either a fast spin-echo sequence or a magnetization-prepared rapid acquisition gradient-echo sequence with repetition time (TR)/echo time (TE)/inversion time (TI)=400–3209msec/3.6–21.9msec/0–1.2sec; slice thickness=3–6.5mm; slice gap=0–2.5mm; number of excitations/averages (NEX)=1–2; matrix size=176–512 × 256–512; and field of view (FOV)= 240–256mm. Diffusion-weighted MR images (DWIs) were acquired before injection of contrast with TE/TR=80–110msec/4–10sec, NEX=1, slice thickness=5 with 0–1mm interslice gap, matrix size=128x128, and FOV=220–256mm using a monopolar spin-echo echo-planar preparation. ADC maps were calculated offline from the acquired DWIs using $b=0$ s/mm² and $b=1000$ s/mm² images. Post-contrast T1-weighted MR images were acquired with identical acquisition parameters shortly after contrast injection with gadopentetate dimeglumine (Magnevist; Berlex), at a concentration of 0.1 mmol/kg, or a contrast agent with equivalent relaxivity. Additional anatomical T2-weighted fast spin-echo and T2-weighted fluid-attenuated inversion-recovery (FLAIR) sequences were also acquired prior to contrast, but not used in the current study. All examinations were acquired within 14 days of starting therapy for all 3 trials, and 29 of the 30 patients used in the cediranib trial received *two* examinations, approximately 1–7 days apart, prior to treatment initiation for the purposes of reproducibility testing.

Contrast-Enhanced T1-Weighted Digital Subtraction Maps (T1 Subtraction Maps)

Contrast-enhanced T1-weighted digital subtraction maps were created by registration, normalization, and subtraction of pre-contrast from post-contrast T1-weighted images as outlined previously (29). Firstly, affine registration was performed between pre- and post-contrast T1-weighted images by using a 12 degree-of-freedom transformation and a correlation coefficient cost function in FSL (FLIRT; FMRIB Software Library, Oxford, England; <http://www.fmrib.ox.ac.uk/fsl/>). Secondly, the image intensities for both pre- and post-contrast T1-weighted images were intensity normalized using custom *c*-code and bash scripts courtesy of the National Institutes of Mental Health Magnetoencephalography 3Core Facility (3dNormalize; NIMH MEG Core, Bethesda, Md; kurage.nimh.nih.gov/meglab/3dNormalize). This normalization was performed by essentially dividing each voxel by the standard deviation of the image intensity from the whole brain [$S_{Nor}(x,y,z)=S(x,y,z)/\sigma_{WB}$], where *S* is raw image signal intensity, *Nor* is normalized, *x,y,z* are voxel coordinates, and *WB* stand for whole brain. Thirdly, voxel-wise subtraction was performed between intensity normalized pre-contrast and post-contrast T1-weighted images (Fig 2A). Lastly, voxels with T1 subtraction values greater than zero were isolated, then manual corrections were made to exclude vessels or erroneous voxels, resulting in final T1 subtraction maps used to extract tumor volumes and act as continuous volumes of interest (VOIs) for ADC histogram analysis (Fig 2C), described below. Any satellite enhancing lesions were pooled together into a single VOI for subsequent analysis.

ADC Histogram Analysis

T1 subtraction-defined enhancing tumor volumes were used to extract ADC values for ADC histogram analysis. Nonlinear regression of a double Gaussian mixed model was then performed for the extracted ADC histograms using GraphPad Prism, Version 4.0c (GraphPad Software, San Diego, California). The model used for the double Gaussian was defined by the following equation:

$$p(ADC)=f \cdot N\left(\mu_{ADC_L}, \sigma_{ADC_L}\right) + (1-f)N\left(\mu_{ADC_H}, \sigma_{ADC_H}\right),$$

where $p(ADC)$ is the probability of obtaining a particular value of ADC in the histogram, *f* is the relative proportion of voxels represented by the lower histogram, $N(\mu,\sigma)$ represents a normal (Gaussian) distribution with mean, μ , and standard deviation, σ , ADC_L represents the lower and ADC_H represents the higher of the two mixed Gaussian distributions (Fig 2D). Resulting model fits were visually inspected and rerun with different initial conditions until adequate convergence was obtained. Goodness of fit was determined to be adequate if the adjusted $R^2 > 0.7$. This approach is similar to those used previously (18–20, 30).

Statistical Analyses and Interpretation

Reproducibility in ADC_L measurements within the enhancing tumor were evaluated by calculating the coefficient of variance (COV) of pre-treatment, double baseline MR examinations acquired as part of the cediranib trial. Also, a paired t-test was used to determine whether a significant difference in ADC_L was observed between these two baseline time points. To determine whether this variability results in meaningful changes in

the classification of ADC_L phenotypes for individual patients, the proportion of patients with the same ADC_L categorization (e.g. high vs. low ADC_L) were calculated as a function of different ADC_L thresholds.

Next, optimal ADC_L thresholds were determined by calculating the Mantel-Haenszel hazard ratio and corresponding *p*-values for patients categorized as “high” vs. “low” ADC_L by changing different ADC_L thresholds. This process was performed for both pooled patients from all trials as well as patients from each trial separately. Using continuous values of volume and ADC_L as well as phenotypes based on these thresholds, log-rank and Kaplan Meier data and Cox proportional hazard models were used to understand the relationship between OS and factors including treatment, patient age, pre-treatment contrast enhancing tumor volume (continuous and dichotomized into large and small sizes using the median volume of the cohort), and ADC_L. Lastly, “risk groups” were defined based on a combination of baseline tumor volume and diffusion MR characteristics. Specifically, tumor volume was dichotomized into large and small sizes, based on the median tumor volume in the sample, and ADC_L phenotypes were defined using the optimized thresholds defined above. We hypothesized a combination of small tumors with high ADC_L measurements would have a significant survival advantage compared with large tumors with low ADC_L measurements when treated with anti-VEGF therapy.

Lastly, using the optimal thresholds defined above, we validated the ability for tumor volume and ADC_L phenotypes to predict response to anti-VEGF therapy by examining an independent cohort of patients treated with either bevacizumab or lomustine monotherapy as part of the BELOB trial. Using continuous values of volume and ADC_L as well as phenotypes based on these thresholds, log-rank and Kaplan Meier data and Cox proportional hazard models were used to test whether volume and ADC_L phenotypes were significant predictors for OS in each of these two therapies.

For all analyses, *P* < 0.05 was considered statistically significant. No corrections for multiple comparisons were performed. Statistical analyses were performed with Stata 12 (2011; College Station, TX) or GraphPad Prism v6.0h (GraphPad Software, Inc., La Jolla, CA). All errors are presented in standard error of the mean (S.E.M.).

RESULTS

Reproducibility of ADC_L Measurements in Recurrent GBM

Repeated (double baseline) ADC measurements prior to initiation of therapy were available for 29 of the 30 patients enrolled in the cediranib trial. Measurements of ADC_L demonstrated a coefficient of variance (COV) of 2.50% ± 0.52% S.E.M. and did not significantly differ between the two evaluations (Fig 3A; *Paired t-test, P=0.4537*). The consistency of ADC_L phenotype classification, defined as the percentage of tumors with the same ADC_L classification at a particular threshold (e.g. high vs. low ADC_L), ranged from 79.3% (23 of 29 with same classification) to 100% (Fig 3B).

Optimized Threshold for Defining ADC_L Phenotypes

An ADC_L threshold of 1.24 $\mu\text{m}^2/\text{ms}$ produced the largest OS differences between patient cohorts when calculating the Mantel-Haenszel hazard ratio and corresponding *p*-values for pooled patients as a function of ADC_L thresholds (Fig 3C–D). This threshold was optimal for the pooled patient cohort, while other thresholds appeared to emerge as specific to the particular anti-VEGF therapy employed (Fig 3E–F). For example, patients treated with cediranib appeared to have the largest difference in OS when using an ADC_L threshold of 1.16 $\mu\text{m}^2/\text{ms}$ and patients treated with cabozantinib had the largest difference using an ADC_L threshold of 1.46 $\mu\text{m}^2/\text{ms}$, while bevacizumab had a relatively constant HR over all ADC_L thresholds evaluated. The consistency of ADC_L phenotype classification using a threshold of 1.24 $\mu\text{m}^2/\text{ms}$, optimal for generalization across all anti-VEGF therapies tested, was approximately 89.7% (26 of 29 with same classification) (Fig 3B) and 55% of these patients had a ADC_L >1.24 $\mu\text{m}^2/\text{ms}$.

Univariate Survival Analysis of Training Data

Log-rank analysis after stratification based on an ADC_L threshold of 1.24 $\mu\text{m}^2/\text{ms}$ confirmed a statistically significant difference in OS (Fig 4A). Notably, patients with high ADC_L had approximately 49% greater OS compared with patients exhibiting a low ADC_L phenotype ($P < 0.0001$, $HR = 0.5303$, median OS = 7.7 vs. 11.6 months). Subsequent univariate analyses of patients within individual treatments showed a significant difference in OS when using a threshold of ADC_L = 1.24 $\mu\text{m}^2/\text{ms}$ in cediranib monotherapy (Fig 4B; $P = 0.0489$, $HR = 0.4980$), bevacizumab monotherapy (Fig 4C; $P = 0.0050$, $HR = 0.4545$), cabozantinib monotherapy (Fig 4D; $P = 0.0107$, $HR = 0.4623$), and aflibercept monotherapy (Fig 4E; $P = 0.0017$, $HR = 0.3313$).

Multivariable Survival Analysis of Training Data

Multivariable Cox proportional hazards analysis considering treatment, patient age, enhancing tumor volume, and continuous estimates of ADC_L using all anti-VEGF treatment naïve patients indicated that age ($P = 0.0140$, $HR = 1.0165$), volume ($P < 0.0001$, $HR = 1.0158$), and ADC_L ($P = 0.0002$, $HR = 0.2555$) were all significant predictors of OS (Table 2). Multivariable Cox regression in patients treated with cediranib using continuous tumor volume and ADC_L phenotype (higher or lower than 1.24 $\mu\text{m}^2/\text{ms}$) suggested age ($P = 0.0156$, $HR = 1.0488$) and ADC_L phenotype ($P = 0.0256$, $HR = 0.3901$), but not tumor volume ($P = 0.0820$, $HR = 1.0131$), were predictive of OS (Table 3). Within patients treated with bevacizumab monotherapy as part of the BRAIN trial, data suggested ADC_L phenotype ($P = 0.0090$, $HR = 0.4495$) was a significant predictor of OS, while volume trended toward significance ($P = 0.0765$, $HR = 1.0157$) and age was not a significant predictor ($P = 0.2492$, $HR = 1.0143$). Enhancing tumor volume ($P = 0.0034$, $HR = 1.0114$) and ADC_L phenotype ($P = 0.0076$, $HR = 0.4195$), but not age ($P = 0.2170$, $HR = 1.0143$), were predictive of OS for patients treated with cabozantinib. In patients treated with aflibercept, tumor volume ($P = 0.0098$, $HR = 1.0353$) was a significant predictor of OS, while ADC_L phenotype trended toward significance ($P = 0.0677$, $HR = 0.4266$).

Since the combined data from all four trials used as a training cohort suggested enhancing tumor volume and ADC_L phenotype were significant, independent predictive factors for OS

in recurrent GBM patients treated with anti-VEGF therapy, three “risk groups” were defined based on a combination of pre-treatment tumor volume and diffusion characteristics. Patients included in the *Risk I* category had the lowest risk, corresponding to small tumors (<25cc) with high diffusivity ($ADC_L > 1.24 \text{ um}^2/\text{ms}$); patients included in the *Risk II* category were defined as having *either* small tumors (<25cc) with low diffusivity ($ADC_L < 1.24 \text{ um}^2/\text{ms}$) *or* large tumors (>25cc) with high diffusivity ($ADC_L > 1.24 \text{ um}^2/\text{ms}$); and patients included in the *Risk III* category were had the highest risk corresponding to large tumors (>25cc) and low diffusivity ($ADC_L < 1.24 \text{ um}^2/\text{ms}$). (Note that patients in the *Risk II* group consisted of both large tumors with high ADC_L and small tumors with low ADC_L , for which there was no difference in OS (*Log-rank*, $P=0.6779$)). Results demonstrate the combination of enhancing tumor volume and ADC_L further enriched the population, with small, high ADC_L tumors showing more than a three-fold longer OS than patients with large, low ADC_L tumors (Fig 4H; $P<0.0001$, $HR=0.2653$, *median OS* = 4.7 vs. 14.9 months).

Validation of ADC_L as a Predictive Biomarker for Anti-VEGF Therapy Using BELOB

To verify ADC_L is a significant, *predictive* imaging biomarker for anti-VEGF therapy, we examined an independent sample of patients from the BELOB trial treated either with bevacizumab or lomustine monotherapy. Multivariable Cox regression analysis including age, continuous measures of tumor volume, and continuous measures of ADC_L (Table 4) showed that volume ($P=0.0008$, $HR=1.0450$) and ADC_L ($P=0.0255$, $HR=0.0764$) were predictive of OS in bevacizumab treated patients, whereas only enhancing tumor volume ($P=0.0034$, $HR=1.0367$), not ADC_L ($P=0.2483$, $HR=0.3553$), was predictive of OS in patients treated with single agent lomustine. Similar trends were observed when examining age, continuous measures of tumor volume, and ADC_L phenotypes using a threshold of $1.24 \text{ um}^2/\text{ms}$ (Table 5). Specifically, results showed that tumor volume ($P=0.0004$, $HR=1.0472$) and ADC_L phenotype ($P=0.0309$, $HR=0.4332$) were predictive of OS in patients treated with bevacizumab, but only tumor volume ($P=0.0019$, $HR=1.0394$) was predictive of OS in patients treated with lomustine. Consistent with trends in the training data, risk categorization based on both tumor volume and ADC_L phenotypes showed a significant difference in OS between *Risk I* and *Risk III* patients treated with bevacizumab (Fig 4G; $P<0.0001$, $HR=0.2093$, *median OS* = 5 vs 10.5 months). Interestingly, a much less dramatic, but still significant, difference in survival was observed between *Risk I* and *Risk III* patients treated with lomustine (Fig 4H; $P=0.0390$, $HR=0.4214$, *median OS* = 6.2 vs. 8.3 mo), likely driven primarily by differences in tumor volume, as *Risk II* patients had a slightly longer median OS compared with other risk categories (*median OS* = 11.2 months in *Risk II* patients treated with lomustine).

DISCUSSION

Results from the current study confirm that pre-treatment diffusion MR characteristics within contrast enhancing tumor are a *predictive* imaging biomarker for overall survival benefit in recurrent GBM patients treated with anti-VEGF therapies. Although these results support previous studies demonstrating the prognostic significance in bevacizumab therapy(18–20), findings from the current study further refine this hypothesis, suggesting

diffusion MR measurements may predict OS during VEGFR-2 inhibition in recurrent GBM, since cediranib, bevacizumab, aflibercept, and cabozantinib all commonly inhibit activity of this receptor. Since VEGFR-2 is thought to be the primary mediator of the pro-angiogenic effects of VEGF on endothelial cells (31–33) and is one of the primary targets for anti-angiogenic therapies in glioblastoma (34), a pre-treatment imaging biomarker that could identify patients who will receive a significant survival benefit from VEGFR-2 inhibition would be valuable for both guiding clinical practice as well as for use in future trials for patient cohort enrichment trials involving anti-VEGF combination strategies.

Data from the current study suggests an ADC_L threshold of $1.24 \text{ um}^2/\text{ms}$ is the optimal threshold for the best prediction of OS when evaluating data pooled from four different anti-VEGF agents that commonly target VEGFR-2, and this threshold for classification maintained similar groupings in more 85% of patients during repeated evaluations 1 week apart (Fig 3A). This optimized threshold is consistent with the previous work by Pope *et al.* (19, 20), who empirically identified a threshold of $1.2 \text{ um}^2/\text{ms}$ for stratifying OS in patients treated with bevacizumab based primarily on the median ADC_L within the datasets evaluated and not based on optimizing prediction of OS. While data from the current study suggests an ADC_L threshold of $1.24 \text{ um}^2/\text{ms}$ may be the optimal threshold for the best prediction of OS when pooling data from all three anti-VEGF agents, Figs 3E–F implies each therapeutic may have their own unique signatures. For example, an ADC_L threshold of $1.46 \text{ um}^2/\text{ms}$ appears to result in the largest difference in OS in patients treated cabozantinib. It is conceivable that the specific mechanisms or domains in which these anti-VEGF agents act may result in different sensitivity to diffusion MR characteristics. Alternatively, these differences may be related to the activity of secondary therapeutic targets in cediranib (e.g. cKIT, PDGFR β) and cabozantinib (e.g. MET, AXL, RET). Although provocative, future studies aimed at further eliciting the possible mechanisms for these observations are necessary to properly test this hypothesis.

The particular mechanism underlying the association between diffusion MRI measures of ADC_L and therapeutic efficacy of anti-VEGF drugs remains speculative. A reasonable explanation for this association may be that tumors with high ADC_L have less total tumor burden, since high diffusivity implies more water content and/or less tumor cellularity (i.e. less tumor cells and more extracellular water). Thus, treatments like anti-VEGF therapy that are known to reduce vascular permeability, and subsequently vasogenic edema, may simply consolidate the total tumor burden by removing excess water. While feasible, this explanation implies pre-treatment ADC_L may be prognostic for all therapies; however, previous studies have failed to identify similar relationships with OS in recurrent GBM treated with chemotherapies including temozolomide or lomustine(18). Additionally, isolation of the lower component of the ADC histogram (i.e. ADC_L) may act to “filter out” the edematous and necrotic portions of the enhancing tumor known to have higher ADC measurements. Hence, ADC_L measurements may be more specific to the composition of tumor and/or stroma within the lesion.

Consistent with this hypothesis, a recent differential gene expression study from our laboratory has identified overexpression of decorin (DCN) as a possible mechanism for this altered water diffusivity (35). DCN may increase water diffusivity through direct modulation

(softening) of the extracellular matrix (ECM), as DCN acts to modulate the rigidity and stiffness of the ECM by binding with various ECM macromolecules and activating specific matrix metalloproteinases (MMPs)(36). The protein core of DCN is known to bind with a variety of collagen molecules, fibrils, and other macromolecules, acting to significantly increase interfibrillary spacing(37). Since ADC is inversely correlated with fluid viscosity (38, 39) and tortuosity of the ECM (40–44), it is conceivable that high DCN expression results in softer, less viscous tumors with decreased boundaries to fluid within the extracellular space from DCM remodeling, ultimately resulting in a higher measured ADC_L . Future studies aimed at exploring the relationship between diffusion MRI and DCN expression, as well as any relationship between DCN expression and OS benefit when treated with anti-VEGF agents, are warranted in order to link these observations and highlight the underlying mechanism behind both water diffusivity changes and therapeutic benefit from anti-VEGF agents.

Study Limitations

The retrospective, multi-center, and international nature of the data in the current study inevitably leads to heterogeneity in MRI acquisition and image quality. However, one may argue this level of heterogeneity more accurately reflects the variability encountered in the real-world, implying diffusion MR may be a robust biomarker suitable for use in clinical practice. We posit a standardized protocol that includes identical T1-weighted pre- and post-contrast scans as well as standardized DWI acquisition, ideally in compliance with the recently outlined *International Standardized Brain Tumor Imaging Protocol* (45), would provide increased consistency and lower variability in T1 subtraction map-defined enhancing tumor volume and ADC estimation. Additionally, image distortions on diffusion MR images obtained using echo planar imaging may have led to inaccuracies when estimating the ADC characteristics within the contrast-enhancing lesion. Estimates of ADC_L , however, have been shown to be relatively robust even in the presence of distortion (30) and results from the current study suggest a COV of only 2.5%, suggesting image distortion may not have been a critical limitation. Additionally, more in-depth baseline characteristics, including information about post-progressive treatment and molecular information, were not available for the trials used in the current study. Recent evidence suggests MGMT promoter methylation status may predict response to bevacizumab (23, 46); however, this information was not available for most trials and this trend has not been confirmed in other anti-VEGF therapies. Also, despite there being little evidence that subsequent treatments have an effect on post-progression survival after failure of anti-VEGF therapies, this is nevertheless a limitation of the current study. Lastly, post-hoc correction for multiple statistical comparisons was not performed, in part due to the exploratory nature of the current study. Despite a relatively large number of comparisons both within and across treatment paradigms, this lack of correction likely did not lead to substantial Type II error, since the effect sizes observed for both volume and ADC_L tended to be large and consistent. Nevertheless, this is a possible limitation to the current study and should be acknowledged.

Conclusion

In summary, the current study suggests diffusion MR characteristics are independent predictors of long-term therapeutic benefit in recurrent GBM treated with anti-VEGF

therapies, including cediranib, bevacizumab, aflibercept, and cabozantinib. Results suggest diffusion MRI signatures can further improve patient stratification, which may be beneficial for future cohort enrichment trials involving anti-VEGF combination strategies and understanding the therapeutic mechanisms that underscore anti-VEGF efficacy and failure.

Acknowledgments

Funding: American Cancer Society (ACS) Research Scholar Grant (RSG-15-003-01-CCE) (Ellingson); American Brain Tumor Association (ABTA) Research Collaborators Grant (ARC1700002)(Ellingson); National Brain Tumor Society (NBTS) Research Grant (Ellingson, Cloughesy); Art of the Brain (Cloughesy); Ziering Family Foundation in memory of Sigi Ziering (Cloughesy); Singleton Family Foundation (Cloughesy); NIH R01CA129371 (Batchelor); NIH R21CA117079 (Batchelor); NIH K24CA125440 (Batchelor)

References

1. Stupp R, Mason WP, van den Bent MJ, Weller M, Fisher B, Taphoorn MJ, Belanger K, Brandes AA, Marosi C, Bogdahn U, Curschmann J, Janzer RC, Ludwin SK, Gorlia T, Allgeier A, Lacombe D, Cairncross JG, Eisenhauer E, Mirimanoff RO. Radiotherapy plus concomitant and adjuvant temozolomide for glioblastoma. *The New England journal of medicine*. 2005; 352:987–96. [PubMed: 15758009]
2. Stupp R, Hegi ME, Mason WP, van den Bent MJ, Taphoorn MJ, Janzer RC, Ludwin SK, Allgeier A, Fisher B, Belanger K, Hau P, Brandes AA, Gijtenbeek J, Marosi C, Vecht CJ, Mokhtari K, Wesseling P, Villa S, Eisenhauer E, Gorlia T, Weller M, Lacombe D, Cairncross JG, Mirimanoff RO. European Organisation for R, Treatment of Cancer Brain T, Radiation Oncology G, National Cancer Institute of Canada Clinical Trials G. Effects of radiotherapy with concomitant and adjuvant temozolomide versus radiotherapy alone on survival in glioblastoma in a randomised phase III study: 5-year analysis of the EORTC-NCIC trial. *The lancet oncology*. 2009; 10:459–66. [PubMed: 19269895]
3. Wen, PY., Cloughesy, TF., Ellingson, BM., Reardon, DA., Fine, HA., Abrey, L., Ballman, K., Bendsuz, M., Buckner, J., Chang, SM., Prados, MD., Pope, WB., Gregory Sorensen, A., van den Bent, M., Yung, WK. Neuro Oncol; Report of the Jumpstarting Brain Tumor Drug Development Coalition and FDA clinical trials neuroimaging endpoint workshop; January 30, 2014; Bethesda MD. 2014. p. vii36-47.
4. Batchelor TT, Mulholland P, Neyns B, Nabors LB, Campone M, Wick A, Mason W, Mikkelsen T, Phuphanich S, Ashby LS, Degroot J, Gattamaneni R, Cher L, Rosenthal M, Payer F, Jurgensmeier JM, Jain RK, Sorensen AG, Xu J, Liu Q, van den Bent M. Phase III randomized trial comparing the efficacy of cediranib as monotherapy, and in combination with lomustine, versus lomustine alone in patients with recurrent glioblastoma. *J Clin Oncol*. 2013; 31:3212–8. [PubMed: 23940216]
5. Friedman HS, Prados MD, Wen PY, Mikkelsen T, Schiff D, Abrey LE, Yung WK, Paleologos N, Nicholas MK, Jensen R, Vredenburgh J, Huang J, Zheng M, Cloughesy T. Bevacizumab alone and in combination with irinotecan in recurrent glioblastoma. *J Clin Oncol*. 2009; 27:4733–40. [PubMed: 19720927]
6. Jensen RL, Ragel BT, Whang K, Gillespie D. Inhibition of hypoxia inducible factor-1alpha (HIF-1alpha) decreases vascular endothelial growth factor (VEGF) secretion and tumor growth in malignant gliomas. *J Neurooncol*. 2006; 78:233–47. [PubMed: 16612574]
7. Plate KH, Breier G, Weich HA, Risau W. Vascular endothelial growth factor is a potential tumour angiogenesis factor in human gliomas in vivo. *Nature*. 1992; 359:845–8. [PubMed: 1279432]
8. Batchelor TT, Reardon DA, de Groot JF, Wick W, Weller M. Antiangiogenic therapy for glioblastoma: current status and future prospects. *Clin Cancer Res*. 2014; 20:5612–9. [PubMed: 25398844]
9. Gerstner ER, Batchelor TT. Antiangiogenic therapy for glioblastoma. *Cancer J*. 2012; 18:45–50. [PubMed: 22290257]
10. Kreisl TN, Kim L, Moore K, Duic P, Royce C, Stroud I, Garren N, Mackey M, Butman JA, Camphausen K, Park J, Albert PS, Fine HA. Phase II trial of single-agent bevacizumab followed

- by bevacizumab plus irinotecan at tumor progression in recurrent glioblastoma. *J Clin Oncol.* 2009; 27:740–5. [PubMed: 19114704]
11. de Groot JF, Lamborn KR, Chang SM, Gilbert MR, Cloughesy TF, Aldape K, Yao J, Jackson EF, Lieberman F, Robins HI, Mehta MP, Lassman AB, Deangelis LM, Yung WK, Chen A, Prados MD, Wen PY. Phase II study of aflibercept in recurrent malignant glioma: a North American Brain Tumor Consortium study. *J Clin Oncol.* 2011; 29:2689–95. [PubMed: 21606416]
 12. Kamoun WS, Ley CD, Farrar CT, Duyverman AM, Lahdenranta J, Lacorre DA, Batchelor TT, di Tomaso E, Duda DG, Munn LL, Fukumura D, Sorensen AG, Jain RK. Edema control by cediranib, a vascular endothelial growth factor receptor-targeted kinase inhibitor, prolongs survival despite persistent brain tumor growth in mice. *J Clin Oncol.* 2009; 27:2542–52. [PubMed: 19332720]
 13. Winkler F, Kozin SV, Tong RT, Chae SS, Booth MF, Garkavtsev I, Xu L, Hicklin DJ, Fukumura D, di Tomaso E, Munn LL, Jain RK. Kinetics of vascular normalization by VEGFR2 blockade governs brain tumor response to radiation: role of oxygenation, angiopoietin-1, and matrix metalloproteinases. *Cancer Cell.* 2004; 6:553–63. [PubMed: 15607960]
 14. Piao Y, Liang J, Holmes L, Henry V, Sulman E, de Groot JF. Acquired resistance to anti-VEGF therapy in glioblastoma is associated with a mesenchymal transition. *Clin Cancer Res.* 2013; 19:4392–403. [PubMed: 23804423]
 15. Lu KV, Chang JP, Parachoniak CA, Pandika MM, Aghi MK, Meyronet D, Isachenko N, Fouse SD, Phillips JJ, Cheresch DA, Park M, Bergers G. VEGF inhibits tumor cell invasion and mesenchymal transition through a MET/VEGFR2 complex. *Cancer Cell.* 2012; 22:21–35. [PubMed: 22789536]
 16. Du R, Lu KV, Petritsch C, Liu P, Ganss R, Passegue E, Song H, Vandenberg S, Johnson RS, Werb Z, Bergers G. HIF1 α induces the recruitment of bone marrow-derived vascular modulatory cells to regulate tumor angiogenesis and invasion. *Cancer Cell.* 2008; 13:206–20. [PubMed: 18328425]
 17. You WK, Sennino B, Williamson CW, Falcon B, Hashizume H, Yao LC, Aftab DT, McDonald DM. VEGF and c-Met blockade amplify angiogenesis inhibition in pancreatic islet cancer. *Cancer Res.* 2011; 71:4758–68. [PubMed: 21613405]
 18. Ellingson BM, Sahebjam S, Kim HJ, Pope WB, Harris RJ, Woodworth DC, Lai A, Nghiemphu PL, Mason WP, Cloughesy TF. Pretreatment ADC histogram analysis is a predictive imaging biomarker for bevacizumab treatment but not chemotherapy in recurrent glioblastoma. *AJNR Am J Neuroradiol.* 2014; 35:673–9. [PubMed: 24136647]
 19. Pope WB, Kim HJ, Huo J, Alger J, Brown MS, Gjertson D, Sai V, Young JR, Tekchandani L, Cloughesy T, Mischel PS, Lai A, Nghiemphu P, Rahmanuddin S, Goldin J. Recurrent glioblastoma multiforme: ADC histogram analysis predicts response to bevacizumab treatment. *Radiology.* 2009; 252:182–9. [PubMed: 19561256]
 20. Pope WB, Qiao XJ, Kim HJ, Lai A, Nghiemphu P, Xue X, Ellingson BM, Schiff D, Aregawi D, Cha S, Puduvali VK, Wu J, Yung WK, Young GS, Vredenburg J, Barboriak D, Abrey LE, Mikkelsen T, Jain R, Paleologos NA, Rn PL, Prados M, Goldin J, Wen PY, Cloughesy T. Apparent diffusion coefficient histogram analysis stratifies progression-free and overall survival in patients with recurrent GBM treated with bevacizumab: a multi-center study. *J Neurooncol.* 2012; 108:491–8. [PubMed: 22426926]
 21. Nowosielski M, Recheis W, Goebel G, Guler O, Tinkhauser G, Kostron H, Schocke M, Gotwald T, Stockhammer G, Hutterer M. ADC histograms predict response to anti-angiogenic therapy in patients with recurrent high-grade glioma. *Neuroradiology.* 2011; 53:291–302. [PubMed: 21125399]
 22. Batchelor TT, Duda DG, di Tomaso E, Ancukiewicz M, Plotkin SR, Gerstner E, Eichler AF, Drappatz J, Hochberg FH, Benner T, Louis DN, Cohen KS, Chea H, Exarhopoulos A, Loeffler JS, Moses MA, Ivy P, Sorensen AG, Wen PY, Jain RK. Phase II study of cediranib, an oral pan-vascular endothelial growth factor receptor tyrosine kinase inhibitor, in patients with recurrent glioblastoma. *J Clin Oncol.* 2010; 28:2817–23. [PubMed: 20458050]
 23. Taal W, Oosterkamp HM, Walenkamp AM, Dubbink HJ, Beerepoot LV, Hanse MC, Buter J, Honkoop AH, Boerman D, de Vos FY, Dinjens WN, Enting RH, Taphoorn MJ, van den Bergmotel FW, Jansen RL, Brandsma D, Bromberg JE, van Heuvel I, Vernhout RM, van der Holt B, van den Bent MJ. Single-agent bevacizumab or lomustine versus a combination of bevacizumab

- plus lomustine in patients with recurrent glioblastoma (BELOB trial): a randomised controlled phase 2 trial. *The lancet oncology*. 2014; 15:943–53. [PubMed: 25035291]
24. Batchelor TT, Sorensen AG, di Tomaso E, Zhang WT, Duda DG, Cohen KS, Kozak KR, Cahill DP, Chen PJ, Zhu M, Ancukiewicz M, Mrugala MM, Plotkin S, Drappatz J, Louis DN, Ivy P, Scadden DT, Benner T, Loeffler JS, Wen PY, Jain RK. AZD2171, a pan-VEGF receptor tyrosine kinase inhibitor, normalizes tumor vasculature and alleviates edema in glioblastoma patients. *Cancer Cell*. 2007; 11:83–95. [PubMed: 17222792]
 25. Sorensen AG, Batchelor TT, Zhang WT, Chen PJ, Yeo P, Wang M, Jennings D, Wen PY, Lahdenranta J, Ancukiewicz M, di Tomaso E, Duda DG, Jain RK. A “vascular normalization index” as potential mechanistic biomarker to predict survival after a single dose of cediranib in recurrent glioblastoma patients. *Cancer Res*. 2009; 69:5296–300. [PubMed: 19549889]
 26. Kim H, Catana C, Ratai EM, Andronesi OC, Jennings DL, Batchelor TT, Jain RK, Sorensen AG. Serial magnetic resonance spectroscopy reveals a direct metabolic effect of cediranib in glioblastoma. *Cancer Res*. 2011; 71:3745–52. [PubMed: 21507932]
 27. Ellingson BM, Kim HJ, Woodworth DC, Cloughesy TF. Contrast-enhanced T1-weighted digital subtraction maps combined with diffusion MRI to identify recurrent glioblastoma patients that benefit from bevacizumab therapy. *J Clin Oncol*. 2014; 32:5s.
 28. Ellingson BM, Harris RJ, Woodworth DC, Leu K, Zaw O, Mason WP, Sahebjam S, Abrey LE, Aftab DT, Schwab GM, Hessel C, Lai A, Nghiemphu PL, Pope WB, Wen PY, Cloughesy TF. Baseline pretreatment contrast enhancing tumor volume including central necrosis is a prognostic factor in recurrent glioblastoma: evidence from single- and multicenter trials. *Neuro Oncol*. 2016
 29. Ellingson BM, Kim HJ, Woodworth DC, Pope WB, Cloughesy JN, Harris RJ, Lai A, Nghiemphu PL, Cloughesy TF. Recurrent glioblastoma treated with bevacizumab: contrast-enhanced T1-weighted subtraction maps improve tumor delineation and aid prediction of survival in a multicenter clinical trial. *Radiology*. 2014; 271:200–10. [PubMed: 24475840]
 30. Woodworth DC, Pope WB, Liau LM, Kim HJ, Lai A, Nghiemphu PL, Cloughesy TF, Ellingson BM. Nonlinear distortion correction of diffusion MR images improves quantitative DTI measurements in glioblastoma. *J Neurooncol*. 2014; 116:551–8. [PubMed: 24318915]
 31. Carmeliet P, Jain RK. Angiogenesis in cancer and other diseases. *Nature*. 2000; 407:249–57. [PubMed: 11001068]
 32. Dvorak HF. Vascular permeability factor/vascular endothelial growth factor: a critical cytokine in tumor angiogenesis and a potential target for diagnosis and therapy. *J Clin Oncol*. 2002; 20:4368–80. [PubMed: 12409337]
 33. Ferrara N. Vascular endothelial growth factor: basic science and clinical progress. *Endocr Rev*. 2004; 25:581–611. [PubMed: 15294883]
 34. Jain RK, di Tomaso E, Duda DG, Loeffler JS, Sorensen AG, Batchelor TT. Angiogenesis in brain tumours. *Nat Rev Neurosci*. 2007; 8:610–22. [PubMed: 17643088]
 35. Pope WB, Mirsadraei L, Lai A, Eskin A, Qiao J, Kim HJ, Ellingson B, Nghiemphu PL, Kharbada S, Soriano RH, Nelson SF, Yong W, Phillips HS, Cloughesy TF. Differential gene expression in glioblastoma defined by ADC histogram analysis: relationship to extracellular matrix molecules and survival. *AJNR Am J Neuroradiol*. 2012; 33:1059–64. [PubMed: 22268080]
 36. Jarvelainen H, Sainio A, Wight TN. Pivotal role for decorin in angiogenesis. *Matrix Biol*. 2015; 43:15–26. [PubMed: 25661523]
 37. Stamov DR, Muller A, Wegrowski Y, Brezillon S, Franz CM. Quantitative analysis of type I collagen fibril regulation by lumican and decorin using AFM. *J Struct Biol*. 2013; 183:394–403. [PubMed: 23747391]
 38. Noda A, Hayamizu K, Watanabe M. Pulsed-gradient spin-echo H-1 and F-19 NMR ionic diffusion coefficient, viscosity, and ionic conductivity of non-chloroaluminate room-temperature ionic liquids. *J Phys Chem B*. 2001; 105:4603–10.
 39. Pearson DS, Strate GV, Vonmeerwall E, Schilling FC. Viscosity and Self-Diffusion Coefficient of Linear Polyethylene. *Macromolecules*. 1987; 20:1133–41.
 40. van der Toorn A, Sykova E, Dijkhuizen RM, Vorisek I, Vargova L, Skobisova E, van Lookeren Campagne M, Reese T, Nicolay K. Dynamic changes in water ADC, energy metabolism,

- extracellular space volume, and tortuosity in neonatal rat brain during global ischemia. *Magn Reson Med.* 1996; 36:52–60. [PubMed: 8795020]
41. Schwartz ED, Cooper ET, Fan Y, Jawad AF, Chin CL, Nissanov J, Hackney DB. MRI diffusion coefficients in spinal cord correlate with axon morphometry. *Neuroreport.* 2005; 16:73–6. [PubMed: 15618894]
42. Beaulieu C. The basis of anisotropic water diffusion in the nervous system - a technical review. *NMR Biomed.* 2002; 15:435–55. [PubMed: 12489094]
43. Nicholson C, Sykova E. Extracellular space structure revealed by diffusion analysis. *Trends Neurosci.* 1998; 21:207–15. [PubMed: 9610885]
44. Sotak CH. Nuclear magnetic resonance (NMR) measurement of the apparent diffusion coefficient (ADC) of tissue water and its relationship to cell volume changes in pathological states. *Neurochem Int.* 2004; 45:569–82. [PubMed: 15186924]
45. Ellingson BM, Bendszus M, Boxerman J, Barboriak D, Erickson BJ, Smits M, Nelson SJ, Gerstner E, Alexander B, Goldmacher G, Wick W, Vogelbaum M, Weller M, Galanis E, Kalpathy-Cramer J, Shankar L, Jacobs P, Pope WB, Yang D, Chung C, Knopp MV, Cha S, van den Bent MJ, Chang S, Yung WK, Cloughesy TF, Wen PY, Gilbert MR. Jumpstarting Brain Tumor Drug Development Coalition Imaging Standardization Steering C. Consensus recommendations for a standardized Brain Tumor Imaging Protocol in clinical trials. *Neuro Oncol.* 2015; 17:1188–98. [PubMed: 26250565]
46. Cloughesy T, Finocchiaro G, Belda-Iniesta C, Recht L, Brandes AA, Pineda E, Mikkelsen T, Chinot OL, Balana C, Macdonald DR, Westphal M, Hopkins K, Weller M, Bais C, Sandmann T, Bruey JM, Koeppen H, Liu B, Verret W, Phan SC, Shames DS. Randomized, Double-Blind, Placebo-Controlled, Multicenter Phase II Study of Onartuzumab Plus Bevacizumab Versus Placebo Plus Bevacizumab in Patients With Recurrent Glioblastoma: Efficacy, Safety, and Hepatocyte Growth Factor and O6-Methylguanine-DNA Methyltransferase Biomarker Analyses. *J Clin Oncol.* 2017; 35:343–51. [PubMed: 27918718]

Translational Relevance

Existing therapies for recurrent glioblastoma (GBM) have only modestly improved survival. Bevacizumab is one of only 3 drugs approved by the FDA for recurrent GBM. Despite favorable early results, subsequent studies in bevacizumab and other anti-VEGF therapies have not found a long-term overall survival (OS) benefit in all patients with recurrent GBM. There are, however, patients who experienced substantial improvement in OS when treated with anti-VEGF therapy. A tool for predicting which patients will have an OS benefit from anti-VEGF therapy would have high clinical and economic impact, as therapies could be withheld until other options have been exhausted. Using data from 5 phase II clinical trials, we demonstrate that diffusion MRI is an independent predictive imaging biomarker for OS in recurrent GBM treated with anti-VEGF therapy, but not chemotherapy. This information can be used for identifying patients for anti-VEGF therapy upon recurrence and for patient selection in future trials.

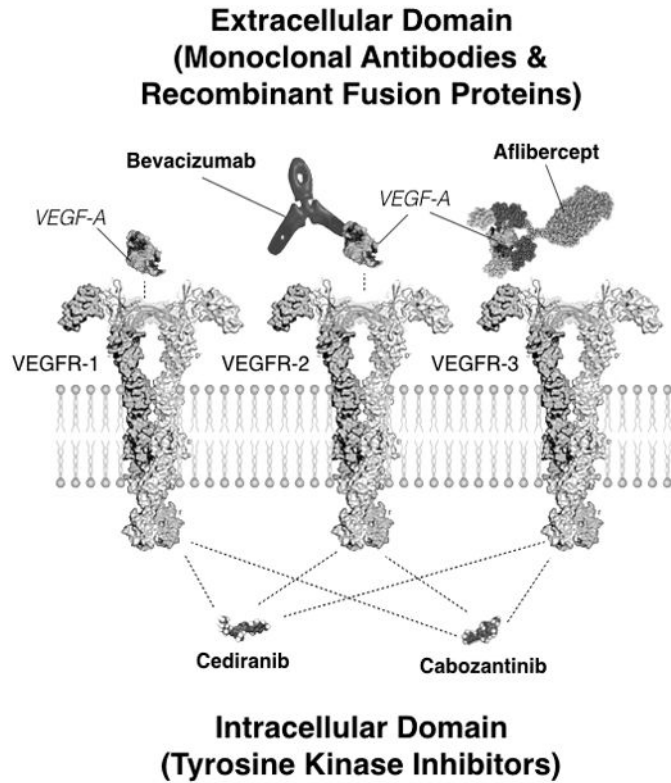


Fig 1. Targets for inhibition of VEGF and VEGFR activity using cediranib, bevacizumab, cabozantinib, and aflibercept

Bevacizumab, a humanized monoclonal antibody for VEGF-A, acts within the extracellular domain to inhibit activity through direct inhibition of circulating extracellular VEGF-A, which reduces activity for both VEGFR-1 and VEGFR-2 receptors. Aflibercept, or “VEGF trap”, is a recombinant fusion protein that sequesters VEGF through use of VEGF-binding portions from extracellular domains of VEGFR-1 and VEGFR-2. Cediranib, a pan-tyrosine kinase inhibitor (TKI), acts in the intracellular domain to primarily inhibit VEGFR-1, VEGFR-2, and VEGFR-3 activity. Cabozantinib, also a TKI, acts within the intracellular domain to inhibit VEGFR-1, VEGFR-2, and VEGFR-3 activity.

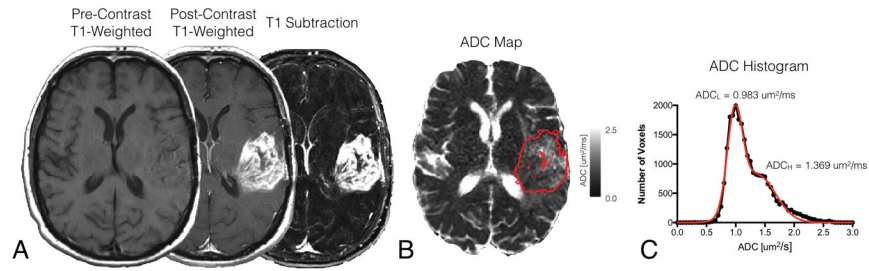


Fig 2. Contrast enhanced T1-weighted subtraction maps and apparent diffusion coefficient (ADC) histogram analysis in a patient with recurrent GBM

A) Pre-treatment pre-contrast, post-contrast, and T1 subtraction maps in a patient with recurrent GBM. B) T1-subtraction defined tumor segmentation overlaid on ADC map. C) Resulting ADC histogram analysis results in the same patient. Note: Black filled circles indicate ADC measurements extracted from contrast enhancing tumor regions. Red line indicates double Gaussian mixed model fit to the underlying ADC histogram.

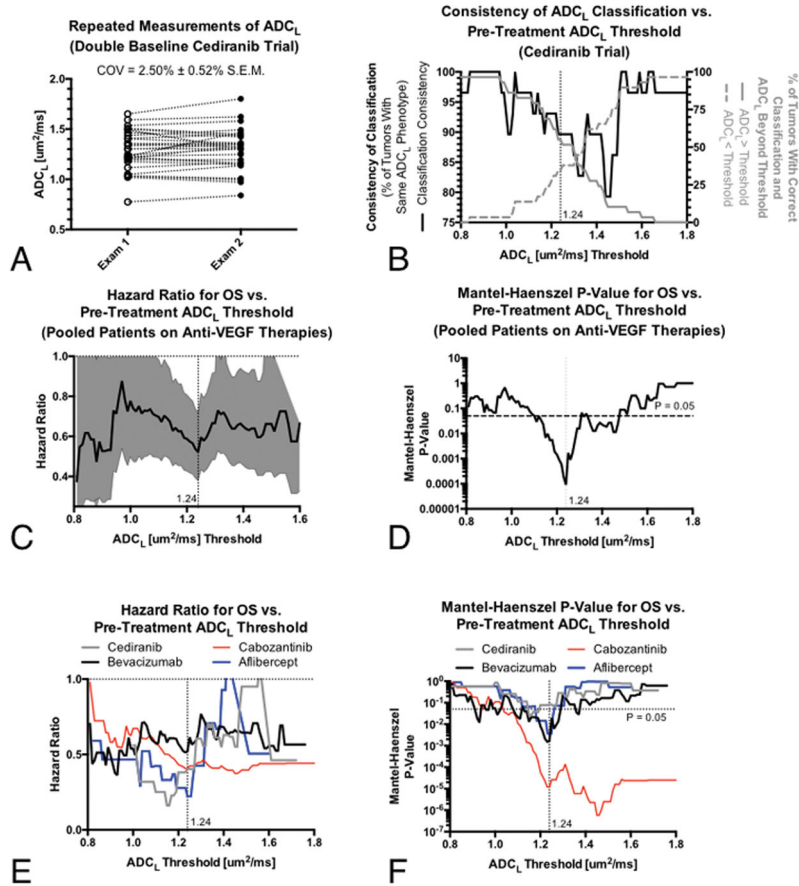


Fig 3. Repeatability of ADC_L measurements, consistency of resulting ADC_L phenotypes for different thresholds, and optimal thresholds for predicting overall survival (OS) in recurrent GBM treated with anti-VEGF therapies

A) Repeated diffusion MR measures of ADC_L in recurrent GBM using “double baseline”, repeated pre-treatment examinations, from the cediranib trial. B) Repeatability of ADC_L phenotypes (e.g. higher vs. lower ADC_L) for different thresholds (solid black line, left y-axis) as well as the proportion of patients higher or lower than this threshold (gray lines, right y-axis). C) Mantel-Haenszel hazard ratios (HRs, solid black line) and 95% confidence intervals (gray area) for OS in recurrent GBM for different ADC_L thresholds in patients pooled from all four anti-VEGF therapies. D) Level of significance (p-values) for OS differences for different ADC_L thresholds in patients pooled from all four anti-VEGF therapies. E) Mantel-Haenszel HRs for OS for different ADC_L thresholds for individual anti-VEGF therapies. F) Level of significance (p-values) for OS differences for ADC_L thresholds in individual anti-VEGF therapies.

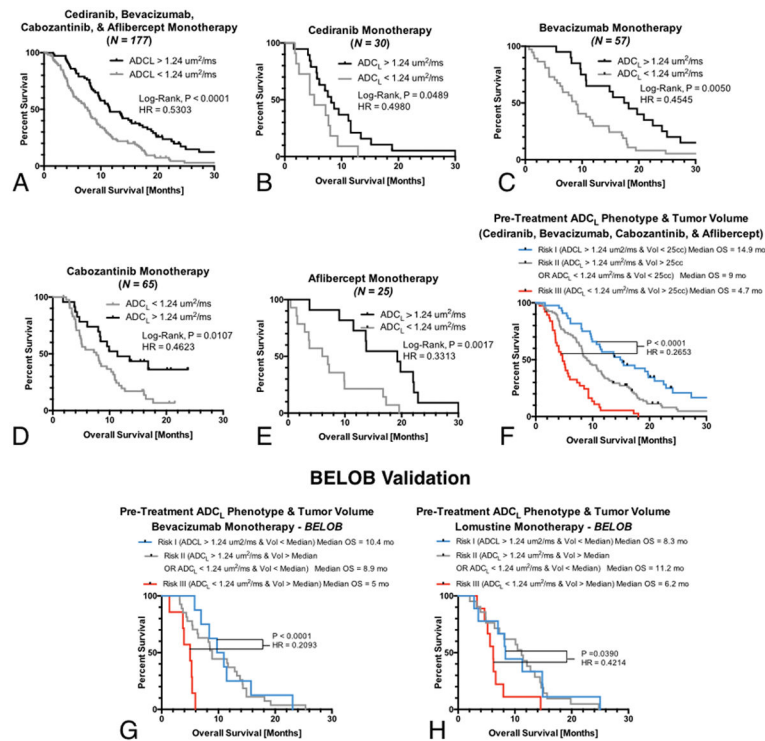


Fig 4. Univariate log-rank survival analysis applied to Kaplan-Meier (KM) curves obtained for pooled and individual anti-VEGF therapies for an optimal ADC_L threshold of 1.24 um²/ms

A) KM data from all anti-VEGF therapies ($P < 0.0001$; $HR = 0.5303$; median OS = 7.7 vs. 11.6 months), B) cediranib ($P = 0.0489$; $HR = 0.4980$; median OS = 5.2 vs. 8.2 months), C) bevacizumab monotherapy ($P = 0.0050$; $HR = 0.4545$; median OS = 9.0 vs. 17.8 months), D) cabozantinib monotherapy ($P = 0.0107$; $HR = 0.4623$; median OS = 7.7 vs. 11.4 months), and E) aflibercept monotherapy ($P = 0.0017$; $HR = 0.3313$; median OS = 6.5 vs. 19.2 months). F) A combination of baseline tumor volume and ADC_L phenotype was a strong predictor of OS in anti-VEGF therapies, with “high risk” patients having large volumes and low ADC_L (Risk III, Median OS = 4.7 months) demonstrating a significantly shorter OS ($P < 0.0001$) compared with “low risk” patients exhibiting small tumors with high ADC_L (Risk I, Median OS = 14.9 months). G) Risk categorization in the BELOB validation cohort suggested a combination of baseline tumor volume and ADC_L was a significant predictor of OS in bevacizumab monotherapy, with “high risk” patients with large volumes and low ADC_L (Risk III, Median OS = 5 months) demonstrating a significantly shorter OS ($P < 0.0001$; $HR = 0.2093$) compared with “low risk” patients exhibiting small tumors with high ADC_L (Risk I, Median OS = 10.4 months). H) The same combination biomarker stratified OS in lomustine monotherapy, but with a smaller difference in median OS between risk categories. “High risk” patients with large volumes and low ADC_L (Risk III, Median OS = 6.2 months) demonstrating a significantly shorter OS ($P = 0.0390$; $HR = 0.4214$) compared with “low risk” patients exhibiting small tumors with high ADC_L (Risk I, Median OS = 8.3 months). Multivariable Cox regression confirmed that tumor volume was a significant prognostic factor for OS in both treatment arms ($P = 0.0004$ for bevacizumab and $P = 0.0019$ for lomustine) but ADC_L

phenotypes were only predictive for bevacizumab therapy ($P=0.0309$ for bevacizumab and $P=0.1455$).

Author Manuscript

Author Manuscript

Author Manuscript

Author Manuscript

Table 1

Patient demographics and cohort data for phase II anti-VEGF trials in recurrent GBM.

	Trial	Number of Patients	Age	Tumor Volume [cc]	ADC_L [$\mu\text{m}^2/\text{ms}$]	Median OS [Months]
Training	Cediranib (NCT00035656)	30	51.8 ± 2.4	35.6 ± 6.1	1.29 ± 0.04	7.6
	Bevacizumab (NCT00345163)	57	51.8 ± 1.5	19.4 ± 2.2	1.18 ± 0.03	10.7
	Cabozantinib (NCT00704288)	65	52.5 ± 1.5	27.5 ± 3.4	1.16 ± 0.03	8.4
	Aflibercept (NCT00369590)	25	54.0 ± 2.2	17.9 ± 3.7	1.18 ± 0.05	9.9
	Total (Pooled) Anti-VEGF Tx Naïve	177	52.4 ± 0.9	24.9 ± 1.9	1.19 ± 0.02	9.3
<i>Training Cohort</i>						
Validation	BELOB (Monotherapy Arms)	81	65.2 ± 1.0	17.7 ± 1.8	1.21 ± 0.03	8.3
	<i>Bevacizumab Monotherapy</i>	42	56.3 ± 1.5	19.6 ± 2.4	1.20 ± 0.03	8.4
	<i>Lomustine Monotherapy</i>	39	56.0 ± 1.4	15.7 ± 2.6	1.22 ± 0.04	8.2

Table 2

Multivariable Cox proportional hazards model results for overall survival in training cohort: Cediranib (NCT00035656), Bevacizumab (BCT00345163), Cabozantinib (NCT00704288), and Aflibercept (NCT00369590)

Variable	Coefficient	Hazard Ratio (95% C.I.)	P-Value
Treatment	-0.1066 ± 0.0769	0.8989 (0.7731 – 1.0451)	0.1656
Age	0.0129 ± 0.0062	1.0130 (1.0007 – 1.0254)	0.0385*
Volume (Continuous)	0.0160 ± 0.0027	1.0162 (1.0108 – 1.0216)	< 0.0001****
ADC _L (Continuous)	-1.2968 ± 0.3323	0.2734 (0.1425 – 0.5244)	0.0001***

Author Manuscript

Author Manuscript

Author Manuscript

Author Manuscript

Table 3

Multivariable Cox proportional hazards model results for overall survival in individual anti-VEGF therapies.

Treatment	Variable	Hazard Ratio (95% C.I.)	P-Value
Cediranib (N = 30)	Age	1.0488 (1.0090 – 1.0901)	0.0156*
	Volume (Continuous)	1.0131 (0.9983 – 1.0282)	0.0820
	ADC _L Phenotype (1.24 um ² /ms threshold)	0.3901 (0.1707 – 0.8913)	0.0256*
Bevacizumab (N = 57)	Age	1.0143 (0.9901 – 1.0391)	0.2492
	Volume (Continuous)	1.0157 (0.9983 – 1.0333)	0.0765
	ADC _L Phenotype (1.24 um ² /ms threshold)	0.4495 (0.2467 – 0.8189)	0.0090**
Cabozantinib (N = 65)	Age	1.0143 (0.9917 – 1.0375)	0.2170
	Volume (Continuous)	1.0114 (1.0038 – 1.0191)	0.0034**
	ADC _L Phenotype (1.24 um ² /ms threshold)	0.4195 (0.2216 – 0.7939)	0.0076**
Aflibercept (N = 25)	Age	1.0079 (0.9735 – 1.0434)	0.6578
	Volume (Continuous)	1.0353 (1.0084 – 1.0628)	0.0098**
	ADC _L Phenotype (1.24 um ² /ms threshold)	0.4266 (0.1710 – 1.0639)	0.0677

Table 4

Multivariable Cox proportional hazard results for overall survival in single agent bevacizumab and lomustine monotherapy (BELOB) using continuous measures of ADC_L.

Treatment Arm	Variable	Coefficient	Hazard Ratio (95% C.I.)	P-Value
Bevacizumab Monotherapy	Age	-0.0037 ± 0.0167	0.9964 (0.9643 – 1.0294)	0.8265
	Volume (Continuous)	0.0440 ± 0.0131	1.0450 (1.0186 – 1.0721)	0.0008***
	ADC _L (Continuous)	-2.5328 ± 1.1341	0.0764 (0.0086 – 0.7335)	0.0255*
Lomustine Monotherapy	Age	0.0108 ± 0.0227	1.0109 (0.9669 – 1.0569)	0.6343
	Volume (Continuous)	0.0360 ± 0.0123	1.0367 (1.0120 – 1.0620)	0.0034**
	ADC _L (Continuous)	-1.0349 ± 0.8965	0.3553 (0.0613 – 2.0591)	0.2483

Author Manuscript

Author Manuscript

Author Manuscript

Author Manuscript

Table 5

Multivariable Cox proportional hazard results for overall survival in single agent bevacizumab and lomustine monotherapy (BELOB) using ADC_L phenotype (threshold of 1.24 $\mu\text{m}^2/\text{ms}$).

Treatment Arm	Variable	Coefficient	Hazard Ratio (95% C.I.)	P-Value
Bevacizumab Monotherapy	Age	-0.0072 \pm 0.0172	0.9928 (0.9600 – 1.0268)	0.6742
	Volume (Continuous)	0.0461 \pm 0.0131	1.0472 (1.0207 – 1.0744)	0.0004***
	ADC _L (1.24 $\mu\text{m}^2/\text{ms}$ threshold)	-0.8365 \pm 0.3875	0.4332 (0.2027 – 0.9260)	0.0309*
Lomustine Monotherapy	Age	0.0116 \pm 0.0233	1.0116 (0.9665 – 1.0589)	0.6194
	Volume (Continuous)	0.0386 \pm 0.0124	1.0394 (1.0143 – 1.0650)	0.0019**
	ADC _L (1.24 $\mu\text{m}^2/\text{ms}$ threshold)	-0.4901 \pm 0.3367	0.6126 (0.3166 – 1.1852)	0.1455

Author Manuscript

Author Manuscript

Author Manuscript

Author Manuscript